Defence Research and Development Canada
Recherche et développement pour la défense Canada

DEFENCE R&D DÉFENSE

Comparison of ALE and SPH methods for simulating mine blast effects on structures

Geneviève Toussaint
Amal Bouamoul
DRDC Valcartier

Defence R&D Canada – Valcartier
Technical Report
DRDC Valcartier TR 2010-326
December 2010

Canada

Comparison of ALE and SPH methods for simulating mine blast effects on structures

Geneviève Toussaint
Amal Bouamoul
DRDC Valcartier

Defence R&D Canada – Valcartier

Technical Report
DRDC Valcartier TR 2010-326
December 2010

Principal Author

Geneviève Toussaint

Defence Scientist

Approved by

Dennis Nandlall

Section Head

Approved for release by

Christian Carrier

Chief Scientist

Abstract

Defence Research and Development Canada – Valcartier (DRDC Valcartier) has been developing protection systems for many years to reduce the vulnerability of light armoured vehicles (LAV) against mine blast. To assist in the development of these protections, experimental tests and finite element (FE) analyses are performed. To carry out these numerical calculations, initial conditions such as the loading prescribed by a mine on a structure need to be simulated adequately. The effects of blast on structures depend often on how these initial conditions are estimated and applied. In this report, two methods were used to simulate a mine blast: the arbitrary Lagrangian-Eulerian (ALE) and the smoothed particle hydrodynamics (SPH) formulations. The comparative study was done for a simple and a more complex target.

The first target is an aluminum plate placed on four steel legs and centred over a surrogate mine filled with 6 kg of C4 which represents a typical buried mine blast scenario. Two FE models were generated: an ALE model and a SPH model. The final deformation of the plate was measured for both approaches and was compared with experimental measurements.

The second target is a mock-up, representing a section of the side of a typical LAV, subjected to a typical improvised explosive device (IED). Two FE models were generated: an ALE model and a SPH model. Parametric studies were done on both models and the best results were compared to the experimental ones. Each comparison included the velocity at the center of the sponson wall, sponson top and sponson sidewall.

R□sum□

Le centre Recherche et d□veloppement pour la d□fense Canada □ Valcartier (RDDC Valcartier) d□veloppe des syst□mes de protection depuis plusieurs ann□es pour r□duire la vuln□rabilit□ des v□hicules blind□s l□gers (VBL) contre les mines □effet de souffle. Pour aider au d□veloppement de ces protections, des tests exp□rimentaux et des analyses par □l□ments finis (EF) sont r□alis□s. Pour effectuer les simulations num□riques, des conditions initiales telles que l□effet de souffle de l□explosion d□une mine sur une structure doivent □tre simul□es ad□quatement. L□effet de souffle de l□explosion d□pend souvent de la fa□on dont les conditions initiales sont estim□es et appliqu□es. Dans ce rapport, deux m□thodes ont □t□ utilis□es pour simuler l□effet de souffle de l□explosion d□une mine : la formulation Lagrangienne Eul□rienne arbitraire (ALE) et la formulation hydrodynamique des particules lisses (SPH). L□□tude comparative a □t□ r□alis□e pour une cible simple et une cible plus complexe.

La premi□re cible est une plaque d□aluminium plac□e sur quatre poutres d□acier et centr□e au-dessus d□une mine simul□e de 6 kg de C4, ce qui repr□sente un sc□nario typique de mine enfouie. Deux mod□les EF ont □t□ g□n□r□s : un mod□le ALE et un mod□le SPH. La d□formation finale de la plaque a □t□ mesur□e pour les deux approches et elle a □t□ compar□e aux mesures exp□rimentales.

La deuxi□me cible est un mod□le partiel repr□sentant une section d□un c□t□ d□un VBL typique, soumis □l□effet de souffle d□un engin explosif improvis□ (EEI) typique. Deux mod□les EF ont □t□ g□n□r□s : un mod□le ALE et un mod□le SPH. Des □tudes param□triques ont □t□ effectu□es pour les deux mod□les et les meilleurs r□sultats ont □t□ compar□s aux r□sultats exp□rimentaux. Pour chacune de ses □tudes, la vitesse au milieu du dessus de l□aile, du mur au-dessus de l□aile et du mur en-dessous de l□aile du mod□le partiel ont □t□ compar□es aux mesures exp□rimentales.

Executive summary

Comparison of ALE and SPH methods for simulating mine blast effects on structures

Toussaint G., Bouamoul A.; DRDC Valcartier TR 2010-326; Defence R&D Canada – Valcartier; December 2010.

Background: Light armoured vehicles (LAV) are exposed to non conventional threats such as improvised explosive devices (IED). To improve the crew survivability, armoured vehicles structures need to be reassessed. To achieve this goal, experimental setups are developed and experimental testing is conducted at the Defence Research and Development Canada – Valcartier (DRDC Valcartier) center to evaluate armoured vehicle structure subjected to blast loadings. In conjunction with these tests, finite element (FE) models are used to optimise the design of protection systems. However, to perform numerical calculations, initial conditions such as the loading prescribed by a mine on a structure need to be simulated adequately. The effects of blast on structures depend often on how these initial conditions are estimated and applied.

Different approaches such as: CONWEP, Westine, CHINOOK and mine pressure model were investigated by DRDC Valcartier to simulate mine blast on structures. The intent of this report is to continue this investigation by evaluating two approaches available in LS-DYNA code: the arbitrary Lagrangian-Eulerian (ALE) and the smoothed particle hydrodynamics (SPH) methods. Two scenarios were simulated: a target plate and a mock-up structure (representing the side of a typical LAV). The numerical results obtained in both scenarios were compared to the experimental results.

Principal results: For the plate setup, both approaches, ALE and SPH, were suitable to simulate the effect of a buried mine. However, SPH is the approach that was in best accordance with the final experimental deformation. In the mock-up scenario, the ALE model better reflected the evolution of the air blast than the SPH model did. The relevant aspects to consider when using the ALE method to model air blast are, to use a fixed domain with a good mesh and to choose judiciously the air material properties and its corresponding equation of state. In general, the factors that may influence an ALE or SPH results are many. Among them are the complexity and dimensions of the structures under the blast, the mesh, the material constitutive models and their corresponding equation of state and the boundary conditions. All these parameters need to be studied in details when modeling blast.

Significance of results: The results obtained in this report will help to better simulate the mine blast effects on different structures using the ALE and SPH methods and consequently, it will improve the analysis of protection systems using FE method.

Sommaire

Comparison of ALE and SPH methods for simulating mine blast effects on structures

Toussaint G., Bouamoul A.; DRDC Valcartier TR 2010-326; R et D pour la défense Canada – Valcartier; Décembre 2010.

Contexte : Les véhicules blindés légers (VBL) sont exposés à des menaces non conventionnelles, telles que les engins explosifs improvisés (EEI). Dans le but d'augmenter la survie des occupants, la structure des véhicules blindés doit être réexaminée. Pour atteindre ce but, des montages expérimentaux sont développés et des tests expérimentaux sont réalisés au centre Recherche et développement pour la défense Canada – Valcartier (RDDC Valcartier) pour évaluer la structure des véhicules blindés soumis au souffle de l'explosion. En même temps, des modèles d'éléments finis (EF) sont utilisés pour optimiser le design de systèmes de protection. Toutefois, pour réaliser les calculs numériques, des conditions initiales telles que l'effet de souffle de l'explosion d'une mine sur une structure doivent être simulées adéquatement. L'effet de souffle de l'explosion dépend souvent de la façon dont les conditions initiales sont estimées et appliquées.

Différentes approches telles que : CONWEP, Westine, CHINOOK et le modèle de pression ont été étudiés par RDDC Valcartier pour simuler l'effet de souffle de l'explosion sur les structures. L'objectif de ce rapport est de poursuivre cette étude en évaluant deux méthodes disponibles dans le code LS-DYNA : la formulation Lagrangienne Eulérienne arbitraire (ALE) et la formulation hydrodynamique des particules lisses (SPH) pour simuler l'effet de souffle de l'explosion d'une mine sur une structure typique. Deux scénarios ont été simulés : une plaque cible et un modèle partiel d'un véhicule blindé (représentant une section d'un côté d'un VBL typique). Les résultats numériques obtenus dans chaque scénario ont été comparés aux résultats expérimentaux.

Principaux résultats : Dans le cas de la plaque cible, les deux approches, ALE et SPH, peuvent être utilisées pour simuler l'effet de souffle d'une mine enfouie. Toutefois, SPH est l'approche dont le résultat était le plus conforme avec la déformation expérimentale finale. Pour le modèle partiel, le modèle ALE a mieux reflété l'évolution du souffle de l'explosion dans l'air que le modèle SPH. Les aspects les plus importants dont il faut tenir compte lorsque le modèle ALE est utilisé pour modéliser un souffle de l'explosion dans l'air sont d'utiliser un domaine fixe avec un bon maillage et de choisir judicieusement les propriétés des matériaux et l'équation d'état correspondante. En général, plusieurs facteurs peuvent influencer les résultats ALE et SPH, notamment, la complexité et les dimensions des structures soumises au souffle de l'explosion, le maillage, les modèles constitutifs des matériaux et leur équation d'état correspondante et les conditions aux frontières. Tous ces paramètres doivent être étudiés en détail lorsqu'on simule l'effet de souffle de l'explosion.

Signification des résultats : Les résultats obtenus dans ce rapport vont aider à mieux simuler l'effet de souffle de l'explosion d'une mine sur différentes structures en utilisant les méthodes ALE et SPH et, par conséquent, cela améliorera l'analyse des systèmes de protection par la méthode des EF.

Table of contents

List of figures

List of tables

Acknowledgements

The authors would like to acknowledge the contribution of Mr. Robert Durocher for the data and information provided on the experimental setup of the mock-up of a typical light armoured vehicle.

This page intentionally left blank.

1 Introduction

Defence Research and Development Canada – Valcartier (DRDC Valcartier) has been developing protection systems for many years to reduce the vulnerability of light armoured vehicles (LAV) to mine blast. To assist in the development of these protection systems, DRDC Valcartier has developed experimental tests and has acquired an expertise in finite element (FE) analyses [*Toussaint and Durocher, 2008, Bouamoul and Gaudreault, 2006, Durocher et al., 2006, Bouamoul and Durocher, 2005, Williams and Fillion-Gourdeau, 2002, Williams et al., 2002, Williams and Poon, 2000, Williams, 1999]*. To perform finite element calculations, initial conditions such as the prescribed loading generated by a mine on a vehicle structure need to be simulated adequately. Accurately simulating the effects of blast on structures often depends on how these initial conditions are estimated and applied.

To simulate the loading conditions generated by mine blast, different approaches were explored in recent years. This report briefly describes these approaches, which include the CONWEP model, the Westine model, the pressure-based mine loading model, the CHINOOK code, the arbitrary Lagrangian-Eulerian (ALE) method and the smoothed particle hydrodynamics (SPH) method. Because each of these techniques has its own limitations, DRDC Valcartier continues to investigate and develop new features to predict mine blast and to model the interaction of blast with different structures.

The aim of this report is to compare numerical results obtained using the two FE formulations ALE and SPH with experimental data. The comparison was done for two scenarios and the results obtained numerically were compared with the experimental data. The first scenario, representing a typical buried mine blast, had an aluminum plate placed on four steel legs and centred over a surrogate mine filled with 6 kg of C4. The experimental setup, the FE models and the results are all given in Chapter 2. The second scenario, a mock-up representing a section of a typical LAV, was subjected to a typical improvised explosive device (IED) air blast. The experimental setup, the FE model and the results are detailed in Chapter 3. For this complex scenario, several parametric studies were conducted for the ALE and SPH methods. For the ALE model, mesh sensitivity analysis of the mock-up and air were conducted. A comparison between a moving and a fixed air domain was done and the effect of the explosive geometry was studied. The effect of the air material properties and equation of state were also investigated. For the SPH model, a mesh sensitivity analysis was conducted and the results obtained with several formulations of the particle approximation theory were compared. Finally, using the best combination of parameters obtained for each models, a comparison was made between the ALE and the SPH finite element results and the experimental data.

This work was done at DRDC Valcartier between June 2007 and September 2010, under the project 12ro03.

1.1 CONWEP model

CONWEP is a collection of conventional weapons effects calculations from the equations and curves of TM 5-855-1 [*Randers-Pehrson and Bannister, 1997*]. In LS-DYNA [*LS-DYNA Keyword User's Manual, 2007*] FE code, the **Load_blast* feature was implemented based on these equations and curves [*Kingery and Bulmash, 1984*] and was used at DRDC Valcartier by Williams *et al*. [2002]. CONWEP model is valid for free air detonation of a spherical charge and for a surface detonation of a hemispherical charge. However, it has some limitations since it considers only the explosive mass but not soil moisture and type.

According to Williams *et al*. [2002], when compared with experiments, the CONWEP model showed poor results that could be explained by the confining effect of the soil. However, the weight of the charge was scaled to fit the experiment and should be rescaled for each new charge. According to Slavik [2009-A], shadowing and focusing of the blast are not taken into account by this model.

1.2 Westine model

The development of the Westine model was based on two charges: 0.0567 kg (1/8 lb) and 0.2268 kg (1/2 lb) [*Westine et al., 1985*]. To use this empirical equation, four criteria which depend on the mine depth of burial, the standoff distance from the centre of the mine, the energy release in the explosive charge, the cross-sectional area of the mine, the lateral distance to the centre of the mine, the soil density and the seismic P-wave velocity in the soil, must be satisfied [*Westine et al., 1985, Tremblay, 1998*]. For typical land mine charges (e.g. 6 kg to 10 kg), the Westine model was extrapolated linearly with respect to the weight of the mine [*Williams et al., 2002*].

The US Army TACOM Impulse model developed by Westine *et al.* [1985] is an improvement from the CONWEP model, since some parameters like the mine depth of burial, charge size, target height, and soil density are taken into account.

The Westine empirical equation was incorporated in MinePre, a software under development at DRDC Valcartier for mine blast loading. The diameter of mine, mine mass, TNT equivalence, location of the centre of the mine, depth of burial and soil density are the parameters that can be used as an input to compute the loading profile. The soil conditions and type are not taken into account by this model.

Williams *et al.* [2002] performed numerical simulations on blast mine effects on armoured vehicles using the Westine model and showed that the impulse loading computed by the model needed to be scaled to fit the experimental results. The authors concluded that it was probably due to some soil conditions that are not taken into account by the model.

The Westine model is useful and accurate for loading a simple geometry like flat plate. However, in cases where the geometry is complex or when complex interactions between the structure and the soil must be taken into account, approaches other than the Westine model need to be considered.

1.3 Pressure-based mine loading model

The empirical equation developed by Westine *et al.* [1985] was used to predict the impulsive loading caused by a landmine detonation. One limitation of this impulse model is its inability to load a FE structure made of solid elements. The pressure-based mine loading model was developed to address this limitation. The pressure model, which is mainly based on the Westine impulse model, uses a pressure time-space distribution to apply the loading conditions on the structure. A series of numerical simulations were conducted to define the appropriate pressure-time history to be applied to elements. The model was also incorporated in the MinePre software.

Due to the limitations of the last three models, other methods like the CHINOOK code, the ALE and the SPH formulations were investigated.

1.4 CHINOOK code

CHINOOK is a computational fluid dynamics (CFD) code developed by Martec Limited [www.martec.com]. It has the ability to model soil effects, which is very important in landmine blast applications, and includes multi-phase material models. Previous studies were performed to compare this CFD model against experimental results [*Donahue et al., 2005, Donahue et al., 2004, Donahue et al., 2003*] and also for design purpose [*Martec Limited, 2006*]. In general, the CHINOOK code has the ability to capture some of the physics involved in the simulation such as the effects of blast clearing, focusing, sheltering and channelling, which simple codes usually cannot do. However, the structure is usually modelled as a rigid body and this code takes more time to run than simple codes.

1.5 ALE method

An alternative to the Lagrangian formulations is to use an arbitrary Lagrangian Eulerian (ALE) formulation to simulate a mine detonation. The ALE formulation has the ability to resolve problems with large mesh distortion [*Donea et al., 2004*]. In this formulation, the reference domain is moving and, a particular case is the Eulerian formulation where the reference domain is fixed. The ALE method is divided into two steps. In the first phase, the mesh is deformed as if it was Lagrangian and in the second phase, called the advection phase, computations at the element boundaries are performed. It is like remapping the deformed mesh to the original fixed mesh [*Alia and Souli, 2006*].

The literature provides different examples of simulation of an explosion using the ALE method using LS-DYNA code [*Cend□n et al., 2007, Li et al., 2007, Larsen and Jorgensen, 2007, Alia and Souli, 2006, Mahmadi et al., 2004, Mullin and O□Toole, 2004, Vulitsky and Karni, 2002, Hilding, 2001, Wang, 2001*]. The ALE method allows for shadowing and focusing of a fluid (e.g. blast, air); however it has some limitations. For example, to accurately capture the shock wave profile, fine mesh must be used; therefore computing time may be very long when large structures are involved or when the explosive is located a few metres from the structure. Another limitation is that there are many parameters in the LS-DYNA code to work with. It is also possible to experience advection errors in the model, which results in leakage into the structure [*LS-DYNA Keyword Users Manual Version 971, 2007*].

Recently, the **Load_blast_enhanced* feature [*Slavik, 2009-A, Slavik, 2009-B and Morten, 2008*] was added to the LS-DYNA code. One option consists in applying the blast pressure profile generated by the feature to the closed ALE air that surrounds the target. It is advantageous to use this capability when the blast source is far from the target because, while still addressing shadowing and focusing of the blast, it is not necessary to model the complete air domain from the blast source to the target, and therefore, the computation time is reduced significantly. Further numerical simulations are required to verify the limitations of this method.

1.6 SPH method

The smoothed particle hydrodynamics (SPH) method was initially developed by Lucy [1977], Gingold and Monaghan [1977] to solve problems in astrophysics [*Bala, 2007*]. Lacome [2000] has implemented this method in LS-DYNA code to avoid problems associated with large mesh deformations and tangling that occurred in high velocity impact problems. In SPH method, the mesh is represented by a set of particles moving like a fluid. To provide the solution of the entire problem, governing equations are resolved for each particle [*Lacome, 2008, Lacome, 2000, LS-DYNA Theory Manual, 2006*].

The SPH approach was used to predict the structural response of a plate to a land mine detonation [*Lacome, 2008*] and to predict the structural response of a mock-up of a typical LAV to an air blast [*Toussaint and Durocher, 2008*]. In these two studies, close correlation with the experiments was achieved with the SPH approach.

2 First scenario: a target plate

2.1 Experimental setup

In order to validate the ALE and SPH approaches, simulations of an experiment performed at DRDC Valcartier, using the experimental blast plate configuration, shown in Figure 1, were performed. A 1.828 m x 1.828 m x 0.03175 m (72 in x 72 in x 1.25 in) aluminum 5083-H131 plate was placed on four steel legs and centred over a surrogate mine containing 6 kg of C4 *[Donahue et al., 2005]*. Lengths of steel tubing having a 1 ft by 1 ft section was placed around the perimeter of the plate. Mass was added to the top of the steel tubing to anchor the apparatus. The mine was buried in a compacted-gravel roadbed with a moisture content of 5% and density of 2300 kg/m^3. The landmine was placed with an overburden of 5 cm and the pressure applied to the plate at a standoff distance of 41 cm was measured. This setup was ideal for a comparison between the ALE and SPH methods because the flat plate loading area and the simple target geometry would not favour one approach over the other.

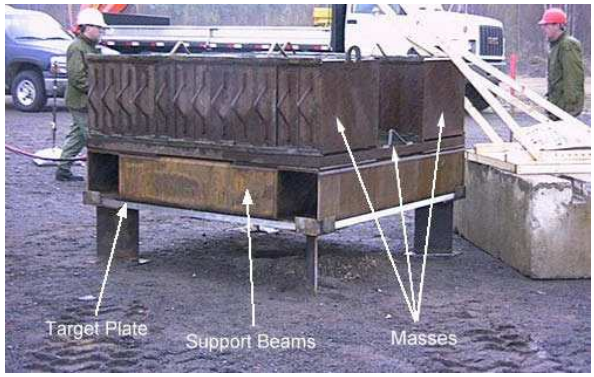

Figure 1: DRDC experimental plate set-up

2.2 Finite element models

The LS-DYNA code was used to model the structural response of the aluminum plate to 6 kg of C4. To reduce the number of elements and nodes and hence the calculation time, only a quarter of the apparatus, as shown in Figure 2, was modelled. This was done in order to take advantage of the planes of symmetry. The ALE and SPH models of the test apparatus developed for this calculation are given in Figure 2.

In both ALE and SPH models, the target (plate) and the steel frame were meshed respectively with 1,296 and 4,024 shell elements. Belytschko-Tsay shell elements were used with five interpolation points through the thickness. Lumped element masses were used to model the added mass on top of the steel tubing.

In the ALE model, the air, soil and mine were modelled respectively with 82,524, 56,936 and 196 hexahedron ALE elements. In the SPH model, the soil and the mine were modelled with 196,010

and 8,000 SPH elements respectively and the default particle approximation was used. A refined mesh was defined for the region of the soil located above the mine.

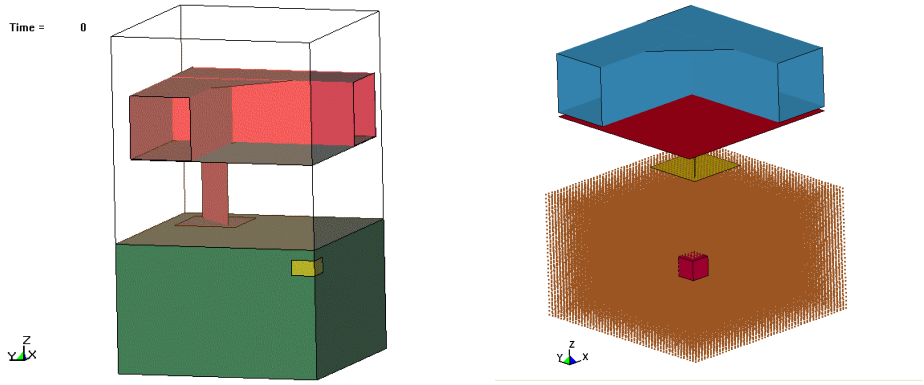

Figure 2: ALE (left) and SPH (right) finite element models

The **Mat_plastic_kinematic* material model was used to model the plate and the frame, and the corresponding material properties are given in Table 1. **Mat_high_explosive_burn* material model and the **JWL* equation of state (EOS) were used for the explosive, and their corresponding properties are provided in Table 2 and Table 3 respectively. **Mat_soil_and_foam_failure* material model was chosen for the soil and **Mat_null* material model with a linear equation of state was used for air. Soil and air material parameters are given in Table 4, Table 5 and Table 6.

Table 1: Material properties used in the experimental setups models

	Armour steel 1	**Armour steel 2**	**Weld***	**Al 5083-H131**
Density, (ρ) kg/m^3	7850	7850	7850	2770
Elastic modulus, (E) GPa	197.5	197.5	197.5	70.33
Poisson□s ratio, (♥)	0.33	0.33	0.33	0.33
Yield stress, (σ_y) GPa	1.0	1.25	1.04	0.322
Tangent modulus, (E_T) GPa	2.175	4.751	1.391	0.34
Failure strain, (ε_f) mm/mm	N/R	N/R	0.225	N/R

* [Bouamoul and Gaudreault, 2006]
N/R: Not required

*Table 2: *Mat_high_explosive_burn material properties [Dobratz and Crawford, 1985]*

	Explosive
Density, (ρ) kg/m^3	1630
Detonation velocity, (D) m/s	6930
Chapman-Jouget pressure, (P_{CJ}) GPa	21

*Table 3: *EOS_JWL equation of state parameters [Dobratz and Crawford, 1985]*

	JWL
A, GPa	371.2
B, GPa	3.231
R1	4.15
R2	0.95
Omeg, (ω)	0.30
Internal energy density, (E_0) GPa - m^3/m^3	7.0
Initial relative volume, (V_0)	1.0

*Table 4: *Mat_soil_and_foam_failure material parameters [Martec Limited, 2007]*

	Soil
Density, (ρ) kg/m^3	1852
Shear modulus, (G) GPa	40.68
Bulk modulus, (K) GPa	50
A0, A1, A2, PC	0.0, 0.0, 1.190, 0.0
VCR, REF	0.0, 0.0
ε1, ε2, ε3, ε4, ε5	0, -0.01861, -0.05616, -0.08934, -0.1276
ε6, ε7, ε8, ε9, ε10	-0.1547, -0.2131, -0.2594, -0.2633, -1.00
P1, P2, P3, P4, P5	0.0, $4.58x10^6$, $1.5x10^7$, $2.92x10^7$, $5.92x10^7$
P6, P7, P8, P9, P10	$9.81x10^7$, $2.894x10^8$, $6.507x10^8$, $6.95x10^8$, $3.753x10^{10}$

*Table 5: *Mat_null material parameters*

	Air set 1	**Air set 2**
Density, (ρ) kg/m^3	1.293	1.293
Pressure cutoff, (P_C) Pa	-100	0

*Table 6: *EOS_linear_polynomial equation of state parameters for the air [Bouamoul and Nguyen-Dang, 2008]*

	Linear polynomial
Polynomial equation coefficient, C0, C1, C2, C3 and C6	0.0
Polynomial equation coefficient, C4 and C5	0.4
Initial internal energy, E_0 (MPa)	0.25
Initial relative volume, V_0	1.0

2.3 Results: comparison between ALE and SPH methods

Figure 3 shows a comparison of the predicted deformation histories between the two numerical models and the experimental test at the same location in the plate. The piezo pins were located 15.24 cm (6 in) from the centre of the plate in the experimental test. The two numerical models predict the same vertical-displacement profile and are in agreement with the experimental data.

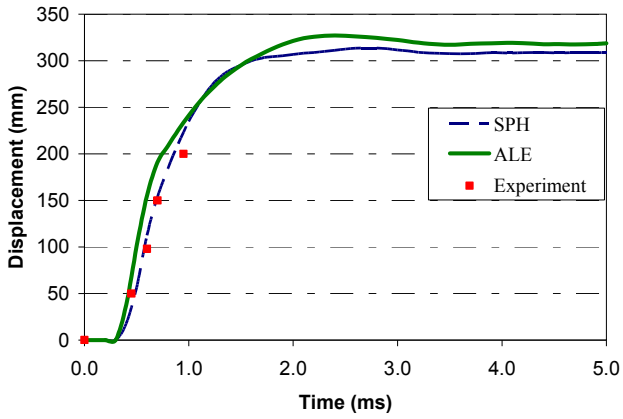

Figure 3: Comparison between the two FE models and the experimental results

The final deformation of the plate was measured after the trial and a maximum deformation of 298 mm was measured. This residual experimental deformation was compared with the output of the two models and they are given in Table 7. The SPH is the approach that is in best accordance with the final experimental deformation.

Table 7: Comparison of centre-plate deformation results

	Deformation (mm)	Relative error
Experimental	298	-
SPH	313	5%
ALE	327	9.7%

2.4 Summary

In this simple scenario, two methods, ALE and SPH, were used to compute the final total deformation of a plate. The same profile for the vertical displacement was obtained for both approaches and was in agreement with experimental data. However, SPH is the approach that was in best accordance with the final experimental deformation.

3 Second scenario: typical LAV mock-up

3.1 Experimental setup

The LAV mock-up is a testing facility developed by DRDC Valcartier to study the reaction of the LAV structure and occupants when subjected to side and under belly blast attacks. Figure 4 shows the mock-up that was developed to conduct full-scale trials and to evaluate the effectiveness of systems such as structural hull reinforcements, add-on armour systems, seating and stowage systems. The mock-up represents a 2-m long section of the rear of a typical Canadian LAV, and for this testing configuration the total mass was 9600 kg. It consists of rigid frames at the front and aft of the mock-up, on which is bolted a sub-assembly undergoing destructive testing and representing the area of interest. For side blast trials, the sacrificial target is a welded assembly of the sidewall, sponson top panel, sponson wall and a section of the floor. The mock-up is equipped with wheels to provide representative geometry and masking.

Figure 4: DRDC Valcartier LAV mock-up testing facility

The mock-up was instrumented with five 3-axis accelerometers mounted on the interior walls (at the centre of the sidewall, at the centre of the sponson top, on the corner of the sponson, at the centre of the sponson wall and at the base of the sponson wall) to monitor the local reaction of the structure. The accelerations obtained experimentally were integrated to generate the velocity history curves, which were compared to numerical results. Also, a laser displacement sensor was aimed at the corner of the sponson. Internal high speed imagery monitored the deformation of the wall and four 3-axis accelerometers were mounted on the roof to measure global motion of the test rig. Wall reflected pressure measurements were taken inside the test rig. External incident pressure measurements were taken at 10 m and 20 m from the charge. Figure 5 shows pictures of the internal instrumentation [*Toussaint and Durocher, 2008*].

Figure 5: Internal instrumentation

3.2 Finite element models

Figure 6 shows the ALE and SPH FE models developed to support the experiments performed on the mock-up [*Toussaint and Durocher, 2008*]. In both models, the sub-assembly parts (mock-up frame) were generated with 2,750 shell elements and the wheels with 1,078 shell elements. The material model used for the mock-up frame was **Mat_plastic_kinematic*. Two types of armour steel were used for these parts and their properties are given in Table 1. The **Mat_high_explosive_burn* material model and the **EOS_JWL* equation of state were used for the explosive, and their corresponding properties are given in Table 2 and Table 3 respectively. The wheels were modelled for masking purposes. The material model **Mat_blatz-ko_rubber* was used to model the wheels, and Table 8 provides their corresponding parameters. In addition, a rigid wall condition was prescribed at the ground level to allow reflection of the ALE air blast and the SPH particles on the ground. Finally, the upper part of the sidewall, the symmetry plane of the floor and both sides of the mock-up were constrained in their 6 degrees of freedom.

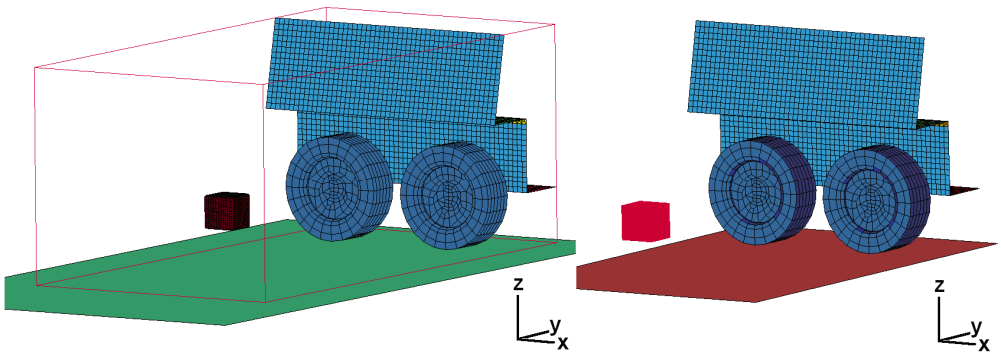

Figure 6: ALE (left) and SPH (right) finite element models

*Table 8: *Mat_Blatz-ko_rubber properties [Bouamoul and Nandlall, 2006]*

	Rubber
Density, (ρ) kg/m^3	1810
Shear modulus, (G) MPa	2.53
Poisson's ratio, ν	0.463

*Table 9: *EOS_ideal_gas equation of state parameters for the air [Martec Limited, 2007]*

	Ideal gas
Nominant constant-volume specific heat coefficient, (C_{v0})	718
Nominant constant-pressure specific heat coefficient, (C_{p0})	1005
Initial temperature, (T_0)	270
Initial relative volume, (V_0)	1

For the ALE model, the air was modelled with 2,833,572 hexahedron ALE elements. The dimensions of these elements were 0.02 m length, 0.02 m width and 0.02 m depth. The model was large enough to enclose the explosive and the mock-up. The **Mat_null* and the **EOS_ideal_gas* equation of state were used to model the air. These properties are summarized in Table 5 and Table 9 respectively. The explosive geometry was defined in the air mesh using the **Initial_volume_fraction_geometry* feature and was modelled with 3,375 hexahedron ALE elements. A **Constrained_lagrange_in_solid* type contact was defined between the ALE elements and the Lagrangian structure. Finally, boundary non-reflecting conditions were used in each side and for the top of the ALE air box to avoid blast wave reflection from each side of the ALE box.

For the SPH model, the explosive was modelled with 215,940 SPH elements. To limit the number of particles to be traced by the simulation and thus enhance the calculation time, a box envelope was specified using the **Control_sph* card. In this way, only the interactions between particles inside this box were considered. Finally, two types of contact were used: **Contact_automatic_nodes* between SPH particles and the mock-up structure and **Contact_automatic_surface* between all the Lagrangian entities.

3.2.1 ALE method

3.2.1.1 Mock-up mesh sensitivity analysis

A mesh sensitivity analysis of the mock-up was done using the ALE method. In the first mock-up mesh, the sub-assemblies (sidewall, sponson top and sponson wall) and the wheels were modelled with 2,750 (0.050 m length on each side of the hexahedron element) and 1,078 shell Belytschko-Tsay elements respectively. The second mock-up mesh contained 9,800 elements (0.025 m length on each side of the hexahedron element) whereas the wheels were meshed with 1078 shell Belytschko-Tsay elements. These two meshes are shown in Figure 7.

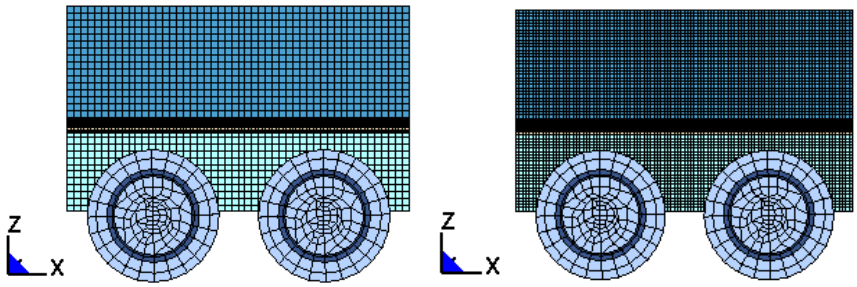

Figure 7: Mesh 1 (left) and mesh 2 (right) of the mock-up

The velocities obtained for the sidewall, sponson top and sponson wall with mesh 1 and mesh 2 were compared to the experimental measurements[1]. Figure 8 shows the sponson wall horizontal velocity (y-axis) according to the axis orientation shown in Figure 7. Figure 9 shows the sponson top vertical velocity (z-axis) and Figure 10 shows the sidewall horizontal velocity (y-axis). Because the time of arrival of the blast was not of interest but only the duration and the maximum velocity, the beginning of the velocity curves were aligned together to make their comparison easier. This alignment was also done for all the following figures of this report.

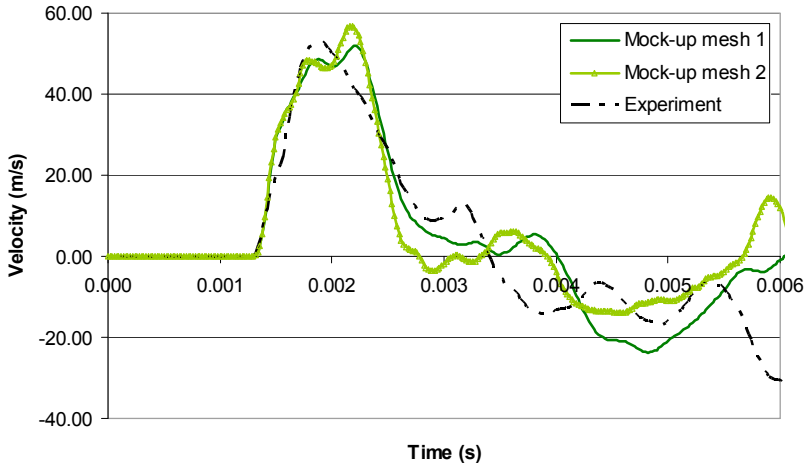

Figure 8: Comparison of the velocity at the centre of the sponson wall between the two mock-up meshes and the experimental results

[1] It is important to mention that the experimental data were obtained from only one field test and therefore, more experimental tests may be needed to average the experimental velocity profile.

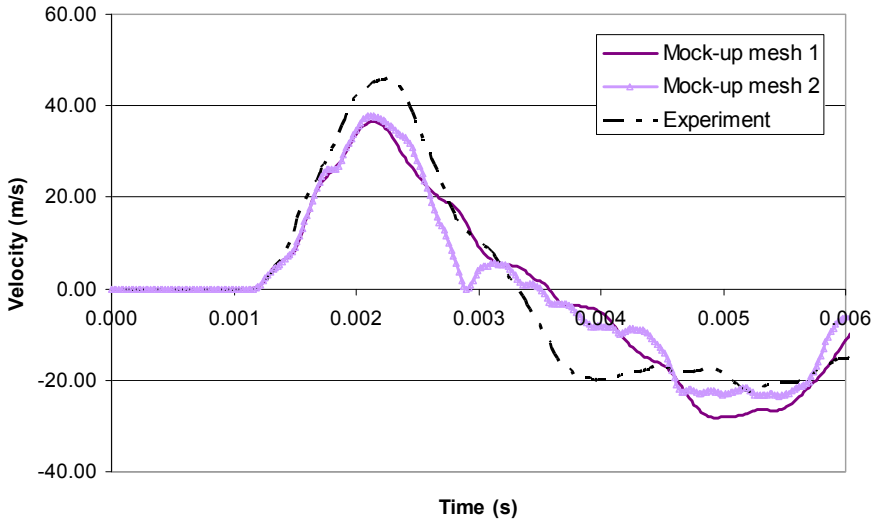

Figure 9: Comparison of the velocity at the centre of the sponson top between the two mock-up meshes and the experimental results

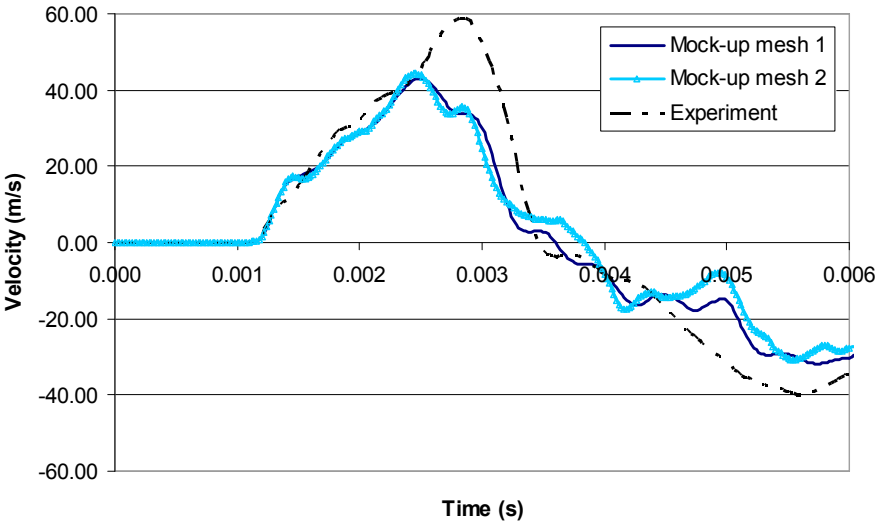

Figure 10: Comparison of the velocity at the centre of the sidewall between the two mock-up meshes and the experimental results

As seen in Figures 8, 9 and 10, the use of coarse and fine meshes gave similar velocity profiles. However, in Figure 10, the numerical peak velocity was approximately 30 percent less than the experimental one. A combination of many parameters may explain this difference: the use of the keyword **Boundary_non_reflecting* on the ALE elements boundary instead of modelling an infinite domain, the air material model and equation of state and the shadowing effect from the wheels. Also, the nodes located on the mock-up boundaries were all fixed in space, which did not

allow any global motion of the mock-up. This was not the case in the experimental trial, where the mock-up was free to move with the blast.

The coarse mock-up mesh was used in the subsequent simulations since both meshes gave similar results. The following section compares two techniques used to simulate the ALE air blast.

3.2.1.2 ALE moving mesh box study

To enhance the calculation time it takes to run the mock-up ALE (Eulerian) simulation, an ALE model with a moving domain reference was generated and compared to a fixed domain (Eulerian). The difference between using fixed and moving domain references is that fewer air elements need to be meshed in a moving domain reference. This could be useful when the standoff distance between the explosive and the structure is large, which means that more air elements are required to enclose all parts in the problem.

The FE model with a moving domain consisted of a smaller ALE box (896,700 hexahedron ALE elements) centred initially at the explosive location. This box, shown in Figure 11, was moving while the explosive was expanding towards the structure. The **Ale_reference_system_group* and **Ale_reference_system_curve* cards were used to allow the translation of this box towards the mock-up. The velocity of the box was adjusted to fit the expansion of the explosive.

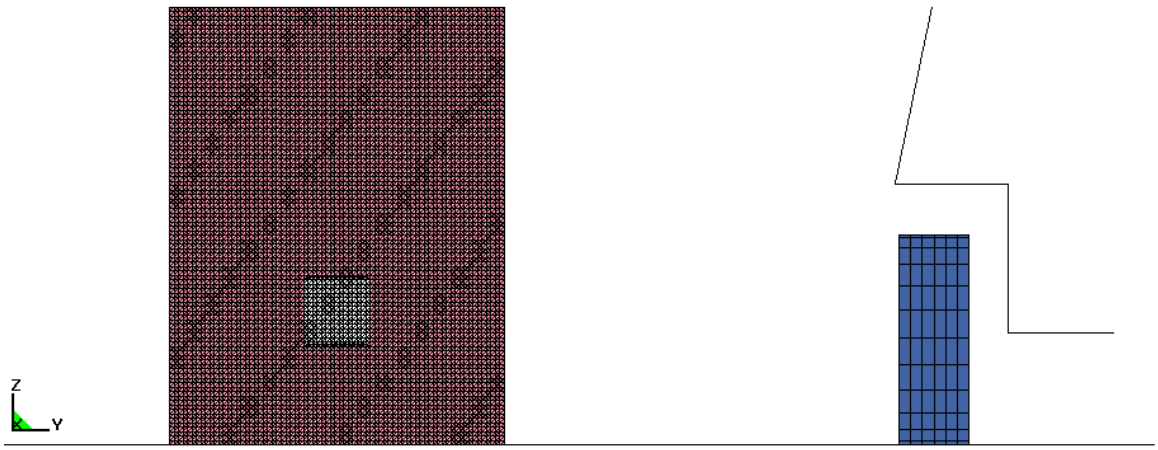

Figure 11: ALE moving mesh

The LS-DYNA version mpp971s R2 7600.1224 and four 32-bit processors were used to perform the ALE moving mesh simulation, while the ALE fixed mesh (Eulerian mesh) simulation was run with one 64b processor and the LS-DYNA version ls971s R2 7600.1224. We expect that the numerical results obtained using these two different platforms (32b versus 64b) and processors (1 versus 4) may be slightly different but still not significantly so.

To verify the accuracy of the results generated with the ALE moving domain and the one generated with a fixed domain, the numerical results were compared to the experimental ones.

Figure 12, Figure 13 and Figure 14 present the velocities obtained at the centre of the sponson wall, sponson top and sidewall of the mock-up in the horizontal (y), vertical (z) and horizontal (y) direction respectively for the fixed mesh, the moving mesh and the experimental results.

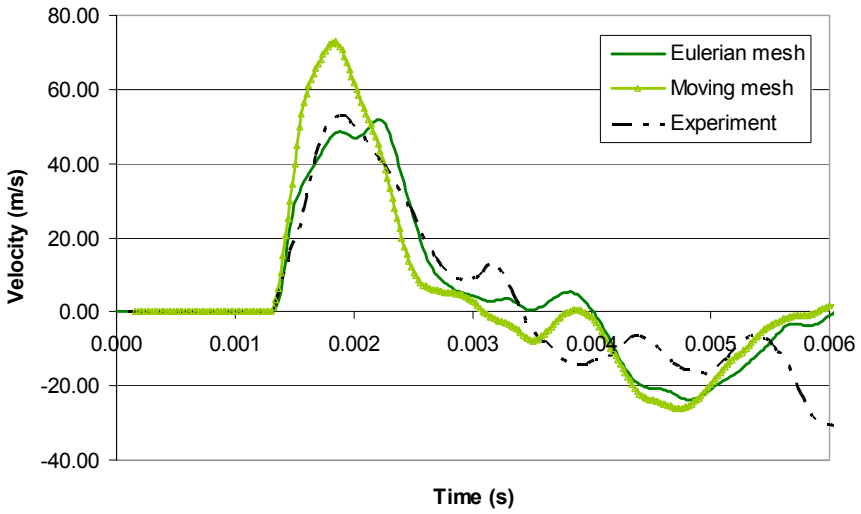

Figure 12: Comparison between the velocity at the centre of the sponson wall for the ALE (fixed and moving mesh) and the experimental results

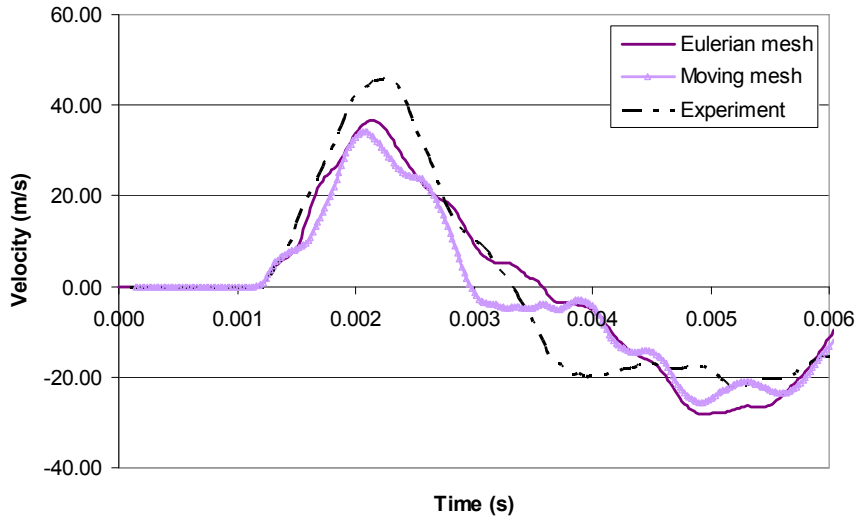

Figure 13: Comparison between the velocity at the centre of the sponson top for the ALE (fixed and moving mesh) and the experimental results

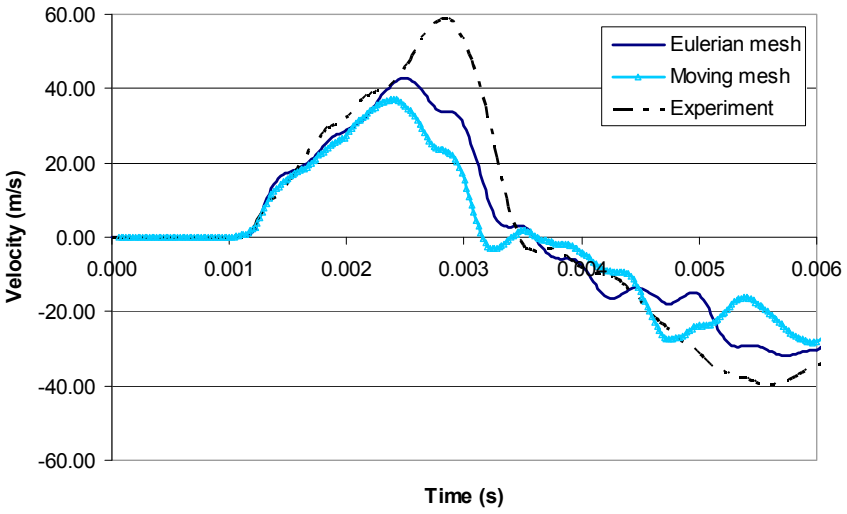

Figure 14: Comparison between the velocity at the centre of the sidewall for the ALE (fixed and moving mesh) and the experimental results

These figures show that the ALE moving mesh slightly underpredicted the velocities of the fixed mesh for the sponson top and sidewall but greatly overpredicted the sponson wall velocities. Consequently, an ALE fixed mesh was used for the future calculations. Annex A gives a summary of the different parameters used in the **Constrained_lagrange_in_solid* card for these calculations.

The next section presents a comparison of three ALE fixed air meshes.

3.2.1.3 Air mesh sensitivity analysis

This section presents a comparison between three different air mesh sizes (mesh 3, mesh 4 and mesh 5)[2] for the ALE fixed mesh. The fifth mesh is the finer one and was the one used previously to perform the mock-up mesh sensitivity analysis and the ALE moving mesh box study. The dimension of the air box was the same in all three meshes but the number of air elements was different. The third mesh contained 355,691 □1 point integration ALE elements with approximate dimensions of 0.04 m length, 0.04 m width and 0.04 m depth. The fourth mesh contained 831,870 □1 point integration ALE elements with approximate dimensions of 0.03 m length, 0.03 m width and 0.03 m depth, and the fifth mesh contained 2,833,572 □1 point integration ALE elements with approximate dimensions of 0.02 m length, 0.02 m width and 0.02 m depth. A cubic geometry was used to model the explosive.

Figure 15, Figure 16 and Figure 17 present, respectively, a comparison between the velocities obtained at the centre of the sponson wall, sponson top and sidewall in the horizontal (y), vertical (z) and horizontal (y) direction for three air meshes and the experimental results.

[2] The air meshes were named mesh 3, mesh 4 and mesh 5 to distinguish from mesh 1 and mesh 2 used for the mock-up meshes.

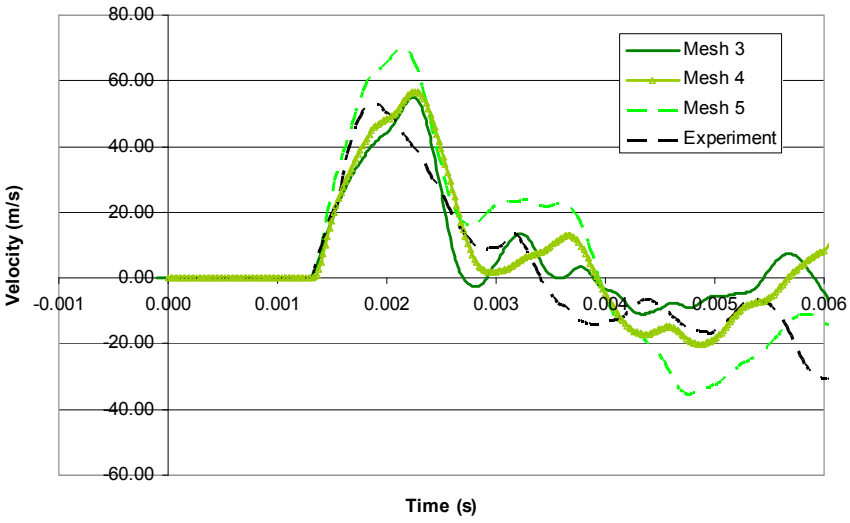

Figure 15: Comparison between the velocity at the centre of the sponson wall for three air meshes and the experimental results

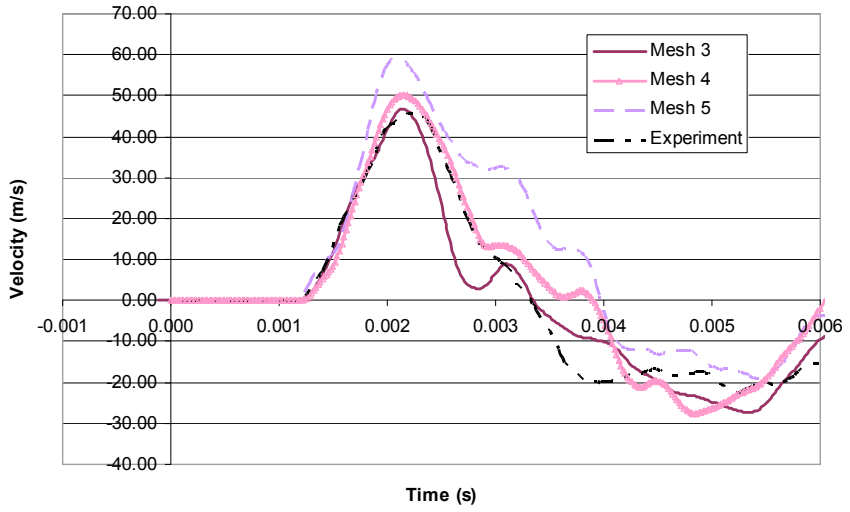

Figure 16: Comparison between the velocity at the centre of the sponson top for three air meshes and the experimental results

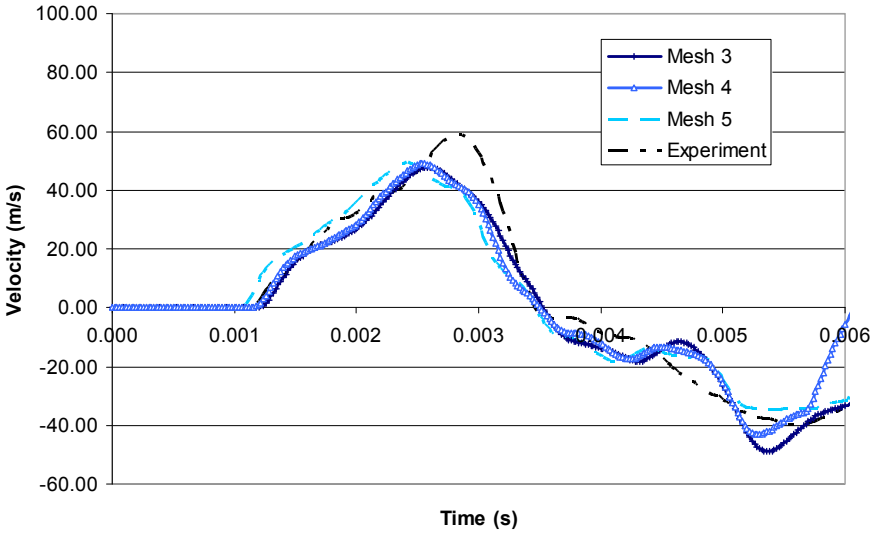

Figure 17: Comparison between the velocity at the centre of the sidewall for three air meshes and the experimental results

As seen in Figure 15 and Figure 16, mesh 3 and mesh 4 provided similar results with maximum peak velocities close to the experimental data while mesh 5 showed a maximum peak velocity higher than the experimental one. Figure 17 showed similar results for the three meshes with peak velocities slightly lower than the experimental one. In general, fine mesh gave better results, however in this case mesh 3 and mesh 4 provided results that better fit with the experimental data. This could be explained by the fact that in mesh 5 the number of coupling points between the ALE and Lagrangian meshes was higher than the one in mesh 3 and mesh 4. According to the LS-DYNA Keyword User's Manual [2007], "Too many coupling points can result in instability, and not enough can result in leakage". Therefore, mesh 5 should not be used in conjunction with the mesh 1 of the mock-up. Other factors that were previously mentioned in Section 3.2.1.1 might have had an influence on the numerical results.

The simulation took 1 hr 23 min. for mesh 3, 6 hrs 49 min. for mesh 4 whereas mesh 5 took 29 hrs 28 min. Therefore, to optimize the time required to run a simulation and considering that mesh 3 and mesh 4 provided similar results, the coarse air mesh (mesh 3) was used in the subsequent analysis.

The next section presents the effect of the explosive geometry.

3.2.1.4 Effect of the explosive geometry

A numerical study was performed to determine if the initial explosive geometry would have had an influence on the reaction of the mock-up. It was expected that the geometry of the explosive should have an influence at close range, but not at long range.

Three different explosive geometries were modelled: cube, sphere and cylinder (L/D = 1). To preserve the total weight of the explosive, the volume of the explosive was used to compute the

dimensions of these three shapes. The FE analyses were performed using the coarse air mesh (mesh 3). Figure 18, Figure 19 and Figure 20 present the velocities obtained at the centre of the sponson wall, sponson top and sidewall of the mock-up in the horizontal (y), vertical (z) and horizontal (y) direction respectively for three different explosive geometries and the experimental results.

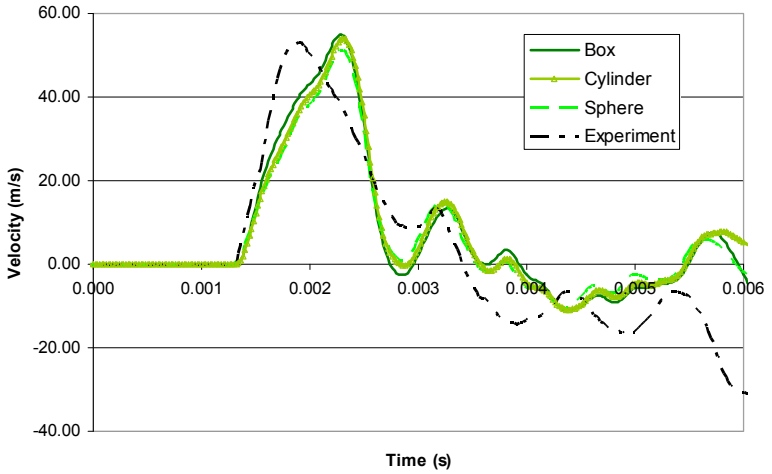

Figure 18: Comparison between the velocity at the centre of the sponson wall for three different explosive geometries and the experimental results

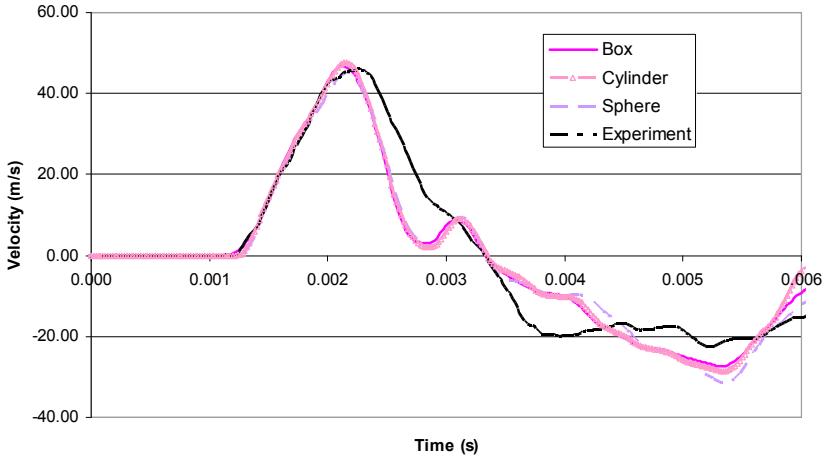

Figure 19: Comparison between the velocity at the centre of the sponson top for three different explosive geometries and the experimental results

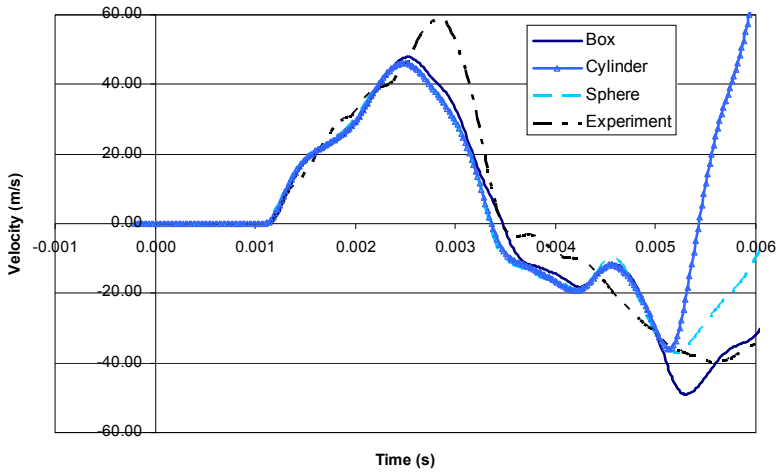

Figure 20: Comparison between the velocity at the centre of the sidewall for three different explosive geometries and the experimental results

From Figure 18, Figure 19 and Figure 20, the geometry of the explosive did not influence the response of the mock-up. The use of the box geometry resulted in slightly higher velocities than with the cylinder or the sphere. If the charge had been closer to the structure, the influence of the geometry would have probably been more important. The cube shape was used for the subsequent FE analyses.

3.2.1.5 Effect of the air EOS parameters and the air pressure cut-off value

The purpose of this section is to compare the results obtained using the **Mat_null* material model using two pressure cut-off values, -100 Pa and 0 (properties are given in Table 5) and to compare the results obtained using two equation of states (EOS): **EOS_linear_polynomial* and **EOS_ideal_gas* (properties are given in Table 6 and Table 9 respectively).

In the LS-DYNA Keyword User's Manual [2007], the **EOS_linear_polynomial* equation of state is defined by equation (1).

$$P = C_0 + C_1\mu + C_2\mu^2 + C_3\mu^3 + (C_4 + C_5\mu + C_6\mu^2)E \quad (1)$$

where $\mu=(\rho/\rho_0)-1$; ρ and ρ_0 are the density and the reference density respectively; C_4 and C_5 are constants to be defined and E is the internal energy defined in unit of pressure. If $\mu<0$ then $C_2\mu$ and $C_6\mu^2$ are set to zero. For an ideal gas, C_0, C_1, C_2, C_3, C_6 are set to zero and equation 1 becomes:

$$P = (C_4 + C_5\mu)E \quad (2)$$

By introducing the value of ρ_0, C_4 *and* C_5 (given in Table 6), equation (2) in the SI system becomes:

$$P = 0.3094\rho E \tag{3}$$

At time equals zero, the initial pressure is computed by introducing the reference density (given in Table 5) and the initial internal energy (given in Table 6), and equals 100.014 kPa.

In the LS-DYNA Keyword User's Manual (2007), the **EOS_ideal_gas* equation of state is defined by equation (4).

$$P = \rho\left(C_p - C_v\right)T \tag{4}$$

where ρ is the reference density (kg/m^3); C_p and C_v are the specific heat capacity at constant pressure and volume respectively (J/(kg·K)) and T is the temperature (K). Assuming that C_p and C_v are constants, $C_p = C_{p0}$ and $C_v = C_{v0}$ and by introducing these values (given in Table 9) in equation (4), equation (4) in the SI system becomes:

$$P = 287\rho T \tag{5}$$

At time equals zero, the initial pressure is computed by introducing the reference density (given in Table 5) and the initial temperature (given in Table 9), and equals 100.195 kPa.

The difference between the initial pressure computed from equation (3) and equation (5) is equal to 0.181 kPa which is negligible (0.18% relative difference between the two pressures). Therefore, similar results are expected when choosing one equation over another in the numerical model.

Table 10 shows a summary of the three simulations parameters. For the first case, the **EOS_ideal_gas* equation of state was used and in the **Mat_null* material model the pressure cut-off value was set to -100 Pa. In the second case, the same EOS was used, but the pressure cut-off value was set to zero and for the third case, the **EOS_linear_polynomial* equation of state was used and the pressure cut-off value was set to zero.

Table 10: EOS and pressure cut-off value for each case

	EOS	**Pressure cut-off value (Pa)**
Case 1	*EOS_ideal_gas*	-100
Case 2	*EOS_ideal_gas*	0
Case 3	*EOS_linear_polynomial*	0

Figure 21, Figure 22 and Figure 23 present the velocities obtained at the centre of the sponson wall, sponson top and sidewall of the mock-up in the horizontal (y), vertical (z) and horizontal (y) direction respectively for the three cases and the experimental results.

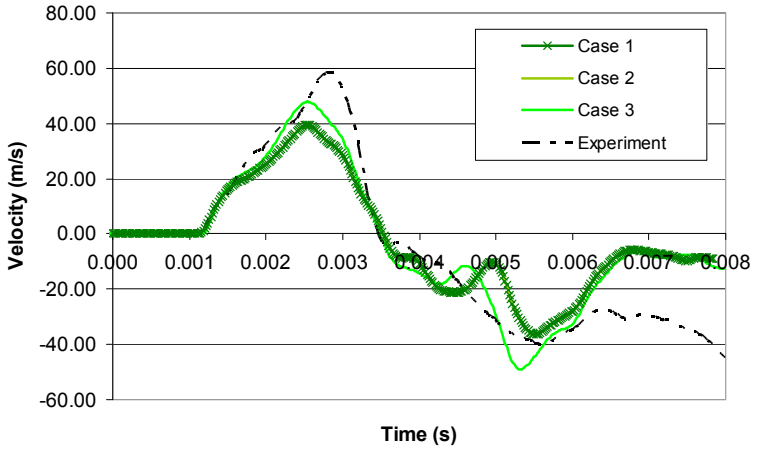

Figure 21: Comparison between the velocity at the centre of the sponson wall for different air set parameters and the experimental results

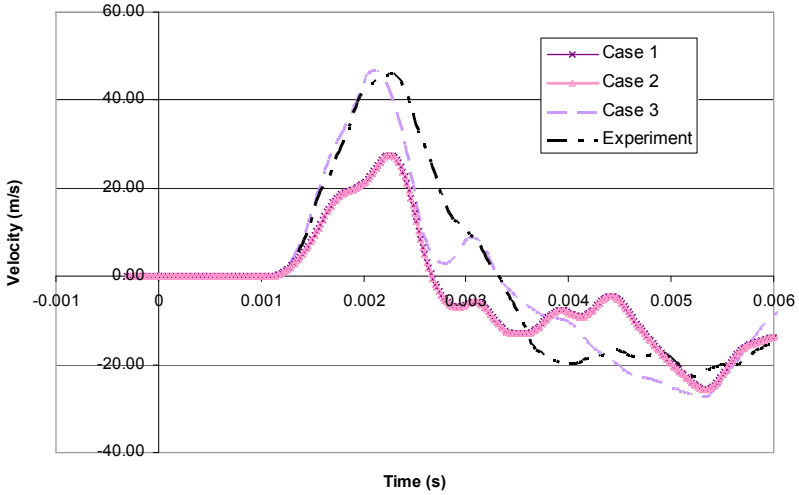

Figure 22: Comparison between the velocity at the centre of the sponson top for different air set parameters and the experimental results

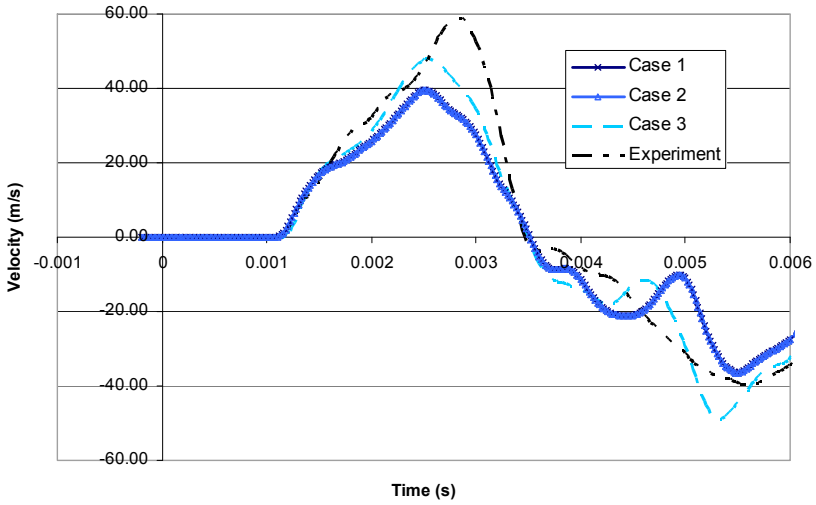

Figure 23: Comparison between the velocity at the centre of the sidewall for different air set parameters and the experimental results

Figure 21, Figure 22 and Figure 23 show that the pressure cut-off value did not influence the results, i.e. in all figures, case 1 and case 2 gave exactly the same velocity profiles. However, contrary to expectations, the results obtained with both EOS were different. The **EOS_linear_polynomial* equation of state predicted higher velocities than the **EOS_ideal_gas* did. According to the LS-DYNA Keyword User's Manual [2007] and for the Eulerian/ALE models, the **EOS_ideal_gas* equation of state preserves the adiabatic state during the advection and therefore, the internal energy is perfectly conserved. This might explain the difference obtained with both EOS. Since we don't have much information about the feature, it is recommended to run an ALE problem with both EOS.

Overall, the pressure cut-off value did not influence the results. Since the FE model with the **EOS_linear_polynomial* equation of state is the one that provided better results compared with the experimental data, it was the one that was chosen in the subsequent analyses.

In summary, the set-up that was selected for the ALE numerical model was: the mock-up mesh 1 (coarse mesh), a fixed ALE domain, the ALE mesh 3 (coarse mesh), box geometry for the explosive and the **EOS_linear_polynomial* equation of state with a pressure cut-off set to zero.

3.2.2 SPH method

To optimise the numerical model using SPH particles, two studies were performed. The first compares three different SPH density meshes and the second compares the results obtained with different particle approximation theories.

3.2.2.1 Effect of the number of SPH particles

A mesh sensitivity analysis was performed using 3,375-SPH (mesh 6), 35,937-SPH (mesh 7) and 215,940-SPH (mesh 8) particles to study the structural deformations of the mock-up. Figure 24, Figure 25 and Figure 26 present the velocities obtained at the centre of the sponson wall, sponson top and sidewall of the mock-up in the horizontal (y), vertical (z) and horizontal (y) direction respectively for the three SPH meshes and the experimental results.

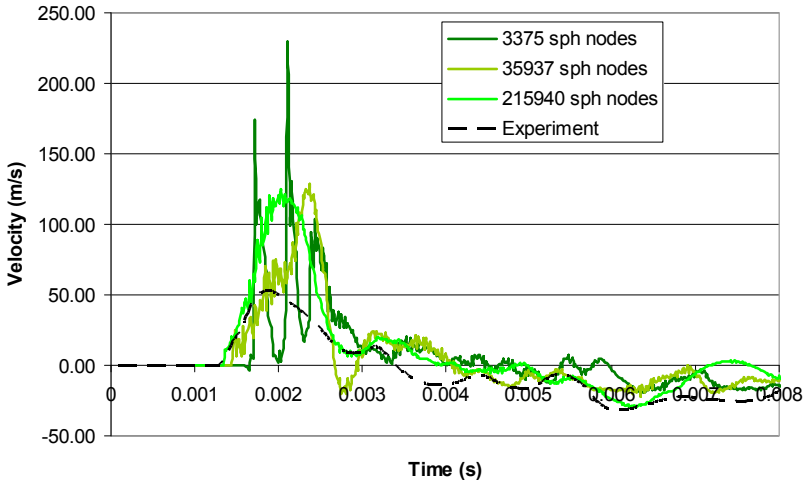

Figure 24: Comparison between the velocity at the centre of the sponson wall for three SPH meshes and the experimental results

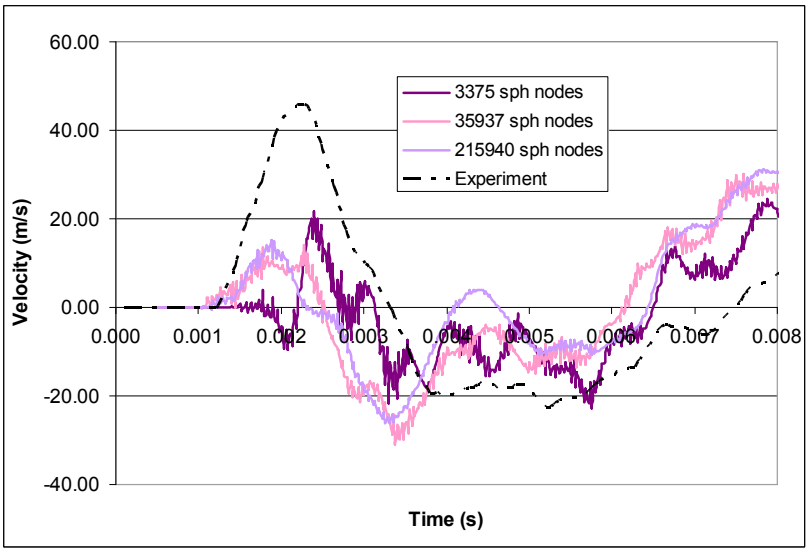

Figure 25: Comparison between the velocity at the centre of the sponson top wall for three SPH meshes and the experimental results

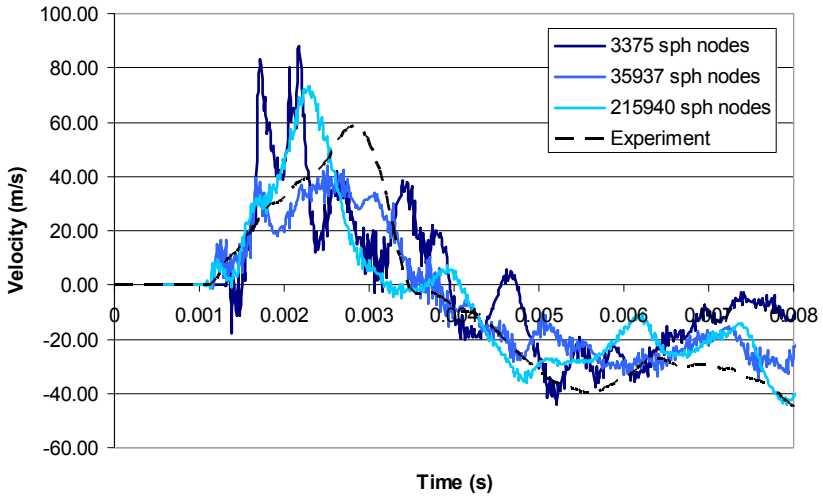

Figure 26: Comparison between the velocity at the centre of the sidewall for three SPH meshes and the experimental results

As seen in Figure 24, 25 and 26, the coarse mesh led to more oscillations of the velocity profiles than the fine mesh did. These oscillations may be the results of the dispersion of the particles near the structure and the local effect of the particles on the structure. Also, the particles did not bypass the wheels like a fluid would do, so it was difficult to reproduce fluid-like behaviour of the blast on the structure. This effect was also observed in the work done by Toussaint and Durocher [2008]. Finally, in this SPH model, the air was not modelled.

The finer mesh (215,940 SPH particles) is the one that provided the best fit with the experiment and thus, was used in the subsequent analysis.

3.2.2.2 Effect of the particle approximation theory

Seven particle approximation theories are available in LS-DYNA code. They are listed in Table 12. All seven formulations were simulated. Formulations 1, 3, 4 and 6 computed infinite velocities, therefore the velocity profiles were only given for formulations 0, 2 and 5. Figure 27 Figure 28 and Figure 29 present the velocities obtained at the centre of the sponson wall, sponson top and sidewall of the mock-up in the horizontal (y), vertical (z) and horizontal (y) direction respectively for the three SPH formulations and the experimental results.

Table 11: Particle approximation theory [LS-DYNA Keyword User's Manual, 2007]

Formulation number	Particle approximation theory	Simulation
0 (default)	Not available	yes
1	Renormalization approximation	no
2	Symmetric formulation	yes
3	Symmetric renormalized approximation	no
4	Tensor formulation	no
5	Fluid particle approximation	yes
6	Fluid particle with renormalization approximation	no

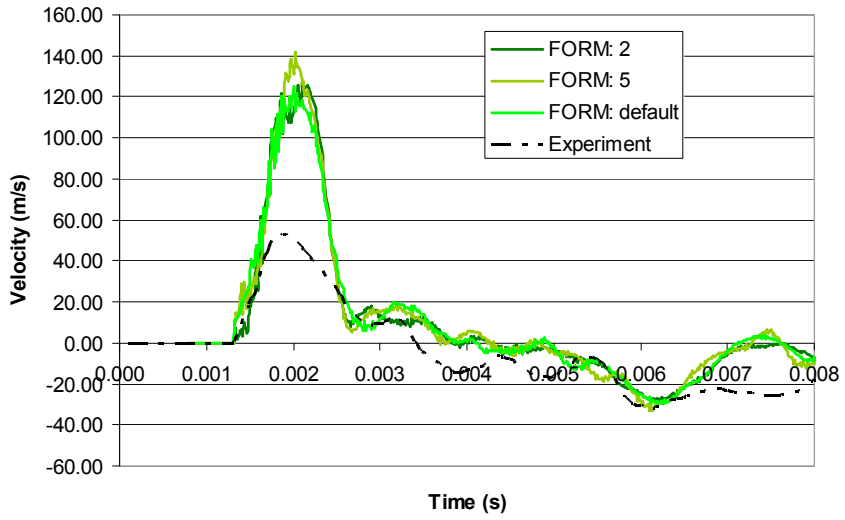

Figure 27: Comparison between the velocity at the centre of the sponson wall for formulation 2, 5 and the default and the experimental results

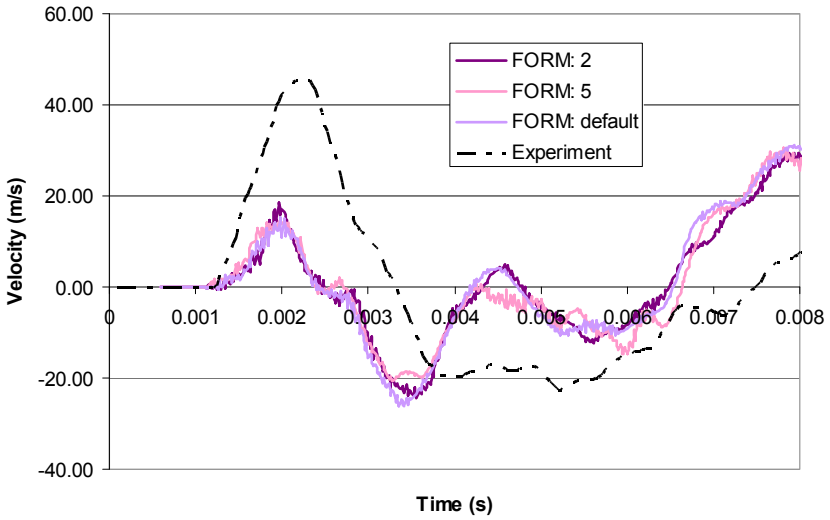

Figure 28: Comparison between the velocity at the centre of the sponson top for formulation 2, 5 and the default and the experimental results

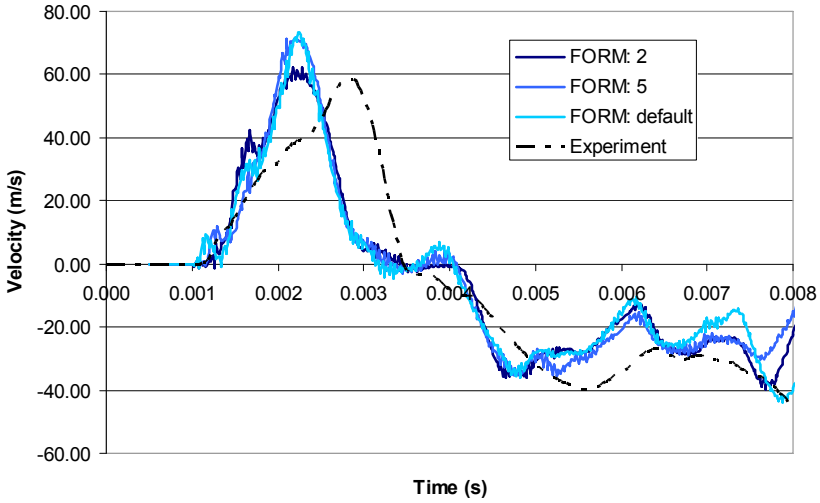

Figure 29: Comparison between the velocity at the centre of the sidewall for formulation 2, 5 and the default and the experimental results

As shown in Figure 27, formulations 0 and 2 gave similar peak velocities and formulation 5 provided the highest peak velocity, but all three formulations computed velocities that were far from the experiment. Some factors that could explain these results were listed in section 3.2.2.1. In Figure 28, all three formulations computed similar peak velocities, but again, they were far from the experimental data. In Figure 29, formulation 2 is the one that was close to the experimental data and thus is the one that provided the best fit with the experimental data.

In summary, the set-up that was selected for the SPH numerical model was: the finer mesh (215,940 SPH particles) and formulation 2 for the particle approximation theory.

3.3 Results: comparison between ALE and SPH methods

To determine which method ALE or SPH was more suitable to model the effect of air blast on a structure, a comparison between the best outcome of the ALE and the SPH formulations was done in this section. The ALE FE analysis was performed using LS-DYNA version ls971s R2 7600.1224 and one processor, whereas the SPH analysis was performed using LS-DYNA version mpp 971s R2 7600.1224 and four processors. The ALE analysis was run on only one processor because of the size of the model (a large amount of memory was necessary to run the analysis). This required running the ALE simulation on a 64b processor and only one 64b processor was available.

For both analyses, the same FE mock-up model (coarse mesh) was used and the explosive was modelled as a box. For the ALE analysis, the ALE coarse mesh was used (355,691 □1 point integration ALE elements) with a fixed domain (Eulerian mesh). A pressure cut-off was set to zero in the **Mat_null* air material model and the **EOS_linear_polynomial* equation of state was used. For the SPH analysis, the numerical simulation was run with an explosive containing 215,940 SPH particles in conjunction with formulation 2 for the particle approximation theory.

It took 1 hr 23 min. to run the ALE problem (coarse mesh) compared to 47 min. for the SPH model (fine mesh).

Figure 30, Figure 31 and Figure 32 show, respectively, the velocity in the horizontal (y) direction at the centre of the sponson wall, the velocity in the vertical (z) direction at the centre of the sponson top and the velocity in the horizontal (y) direction at the centre of the sidewall of the ALE and SPH numerical model results compared to the experimental data.

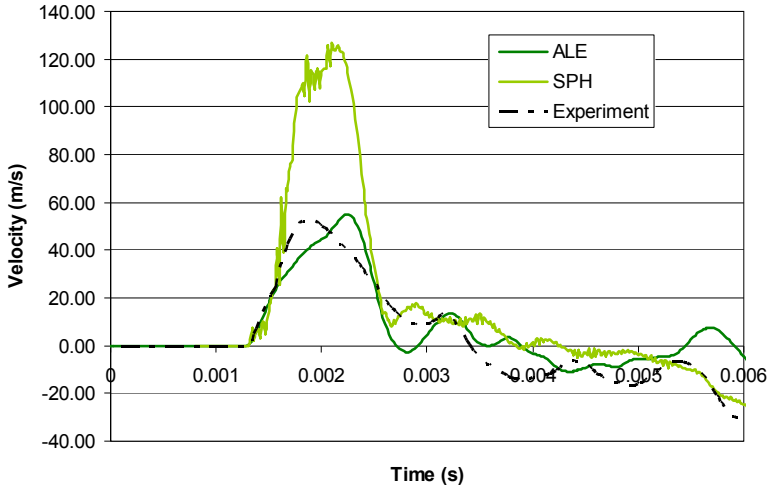

Figure 30: Comparison of the velocity at the centre of the sponson wall for ALE, SPH and the experimental results

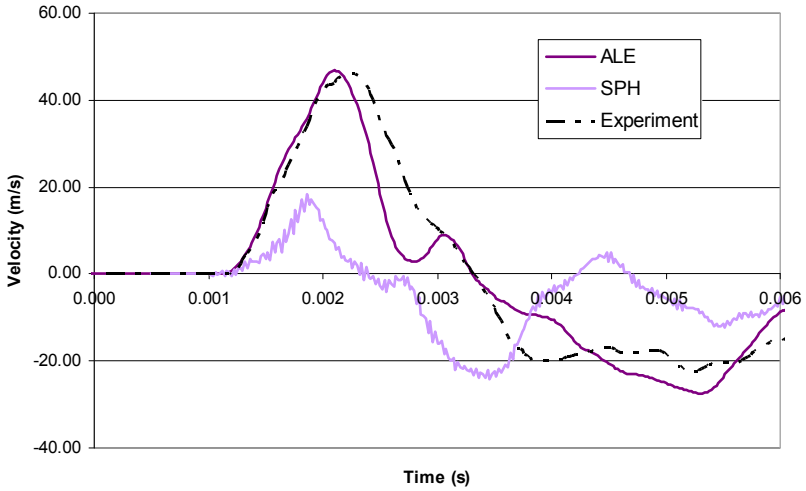

Figure 31: Comparison of the velocity at the centre of the sponson top for ALE, SPH and the experimental results

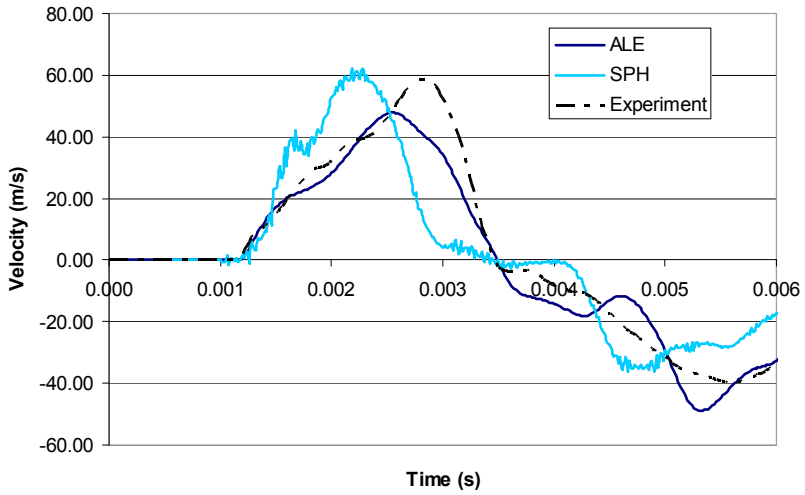

Figure 32: Comparison of the velocity at the centre of the sidewall for ALE, SPH and the experimental results

The SPH model overpredicted the sponson wall peak velocity and underpredicted the sponson top peak velocity compared to the experimental results. The sidewall peak velocity was similar to the experimental results. The ALE model gave similar peak velocities for the sponson wall and sponson top but underpredicted the sidewall peak velocity. Overall, the velocities obtained with the ALE model were closer to the experimental velocities than those obtained with the SPH model. Some factors could explain these results. In the SPH meshless formulation when particles are far from each other, some numerical instability may occur. This effect was emphasized in the second scenario where the blast was far from the structure. Also, shadowing is not accounted for when using SPH formulation. Also, the air was not modelled in the SPH

model. For all these reasons, SPH is probably not the accurate approach to use when the air blast is far from the structure.

3.4 Summary

In the mock-up scenario, different numerical analyses were performed for both methods. For the ALE model, initially a mesh sensitivity analysis of the mock-up was done and since both meshes were in agreement with the experimental data, the coarse mesh of the mock-up was the one that was used in the subsequent analyses. A comparison between moving and fixed ALE air meshes was done and it was shown that for the current application, it was more appropriate to use an ALE fixed mesh (Eulerian mesh). Also, the effect of air element size was studied and the coarse air mesh (mesh 3) was chosen. Then the effect of the explosive geometry was simulated, and it was shown that for this particular experimental trial and with the actual standoff distance, the geometry of the explosive did not significantly influence the response of the mock-up. Finally, the effect of air material properties, especially the pressure cut-off, and the equation of state were investigated. It was demonstrated that for the ALE model, the value of the pressure cut-off in the material model did not influence the results. However, different results were obtained with the **EOS_linear_polynomial* and the **EOS_ideal_gas* equations of state. The **EOS_linear_polynomial* was chosen since it provided results that were closer to the experimental data. An SPH mesh sensitivity analysis was performed and showed that a fine mesh (215,940-SPH particles) was necessary to simulate a fluid-like behaviour and to avoid local effects (i.e. when particles are too large, they impact shell elements and create local holes instead of creating a global deformation of the structure). Also, three particle approximation theories were investigated and formulation 2 is the one that provided best results.

Factors other than the one presented in this study could have influenced the numerical results. For example, blast shadowing was dependent on how the wheels were modelled (dimensions and properties) and thus could have an influence on the numerical results. Also, the nodes located at the outside boundaries of the mock-up were all fixed in space, which did not allow any global motion of the structure (only the local reaction was studied in this work). This was not the case in the experimental trial, where the mock-up was free to move with the blast.

Finally, the best results obtained for each method were compared and it was shown that the ALE formulation reflected the expansion of the air blast better than the SPH did. Also, since only one set of experimental data was generated so far, additional tests under the same conditions would be required to assess the experimental variation.

4 Conclusion

One major issue for numerical analysis is to accurately predict the mine blast effects on light armoured vehicles (LAV). Therefore, two approaches were evaluated in this report: smoothed particle hydrodynamics (SPH) and arbitrary Lagrangian Eulerian (ALE) formulations to simulate a mine blast on a typical structure. Two scenarios were studied using these two methods.

In the target plate scenario, the same vertical-displacement profile was obtained for both ALE and SPH approaches and was in agreement with experimental data. However, SPH is the approach that was in best accordance with the final experimental deformation.

In the mock-up scenario, many studies were performed but in general the ALE model reflected the evolution of blast better than the SPH model did.

The more relevant aspects to consider when using the ALE method to model an air blast are to use a fixed domain with a good mesh and to carefully choose the air material properties and its corresponding equation of state.

In general, many factors may influence ALE or SPH finite element results. They include: the complexity and dimensions of the structures exposed to the blast, the mesh, the material constitutive models and their corresponding equation of state and the boundary conditions. All these parameters need to be investigated in more detail when simulating a mine blast. Also, since only one set of experimental data was generated so far for the mock-up, additional experimental tests under the same conditions would be required to assess the experimental variation.

More work needs to be done in order to determine the accurate loading to be used for landmine and air blast scenarios. Further numerical simulations and experiments should be performed to get a more thorough study on the ALE and the SPH approaches. In particular, it would be important to compare not only the local reaction of the finite element structure with experimental data but also the global motion. Also, an investigation on the new feature available in LS-DYNA that combines the **Load_blast_enhanced* card and the ALE method could be relevant. Finally, it would be of interest to test the ability of the CHINOOK code to model landmine scenarios.

References

Alia A. and Souli M. (2006). *High Explosive Simulation Using Multi-Material, Applied Thermal Engineering 26:1032-1042*.

Bala S. (2007) *Smooth Particles Hydrodynamics in LS-DYNA*, Powerpoint presentation, Livermore Software Technology Corporation.

Bouamoul A. and Durocher R. (2005). *Numerical simulations of LAV III Subject to detonation of blast landmines – Baseline analysis of detonation under the third and fourth wheels*. (DRDC Valcartier TM 2005-343). Defence R&D Canada Valcartier. Confidential.

Bouamoul A. and Gaudreault P. (2006). *A simplified method of modeling welds in light armoured vehicles subjected to an anti-vehicular blast loading*. (DRDC Valcartier TM 2006-121). Defence R&D Canada Valcartier. Unclassified.

Bouamoul A. and Nandlall D. (2006). *Modelling of the hydrodynamic RAM effect in the Bell Helicopter Canada composite wing box struck by a 23-mm high explosive incendiary and armour-piercing incendiary rounds*. (DRDC Valcartier ECR 2006-100). Defence R&D Canada Valcartier. Unclassified.

Bouamoul A. and Toussaint G. (2008). *Experimental tests and numerical calculations using ALE and SPH approaches on mine blast effects on structure*, 24th International Symposium on Ballistics, New Orleans.

Bouamoul A and Nguyen-Dang T.V. (2008). *High explosive simulation using arbitrary Lagrangian-Eulerian formulation*. (DRDC Valcartier TM 2008-254). Defence R&D Canada Valcartier. Unclassified.

Cend□n D. A., G□lvez F., Enfedaque A. and S□nchez-G□lvez V. (2007). *Analysis of armoured vehicles blast protection by using finite element codes*, 23rd International Symposium on Ballistics.

Dobratz B.M. and Crawford P.C. (1985). *Properties of Chemical Explosives and Explosive Simulants*, UCRL-52997 Change 2, Lawrence Livermore National Laboratory.

Donea J., Huerta A., Ponthot J.-Ph, Rodriguez-Ferran A. (2004). *Chapter 14: Arbitrary Lagrangian-Eulerian Methods*, Encyclopedia of Computational Mechanics, Vol.1: Fundamentals, www.wiley.co.uk/ecm/pdfs/Volume_1_Chapter14.pdf .

Donahue L., Link R., Josey T., Hlady S., Bergeron D., Durocher R. and Williams K. (2003). *Structural Response to Land Mines*, 74th Shock and Vibration Symposium, San Diego, USA.

Donahue L., Hlady S. and Link R. (2004). *Numerical Modelling of Soils Subjected to Explosive Loading*, 18th International Symposium on the Military Aspects of Blast and Shock, Bad Reichenhall, Germany.

Donahue L., Bouamoul A. and Dunbar T.E. (2005). *Numerical Modeling Approaches for Simulation of Landmine Blast Loading*, 76th Shock and Vibration Symposium, Destin, USA.

Durocher R., Bouamoul A., Roberts W. and St-Jean B. (2006). *MGS mine protection study phase*. (DRDC Valcartier TM 2006-401). Defence R&D Canada Valcartier. Confidential.

Gingold R.A. and Monaghan J.J. (1977). *Smoothed particle hydrodynamics: theory and application to non-spherical stars*, Monthly Notices of the Royal Astronomical Society.

Hilding D. (2001). *Simulation of a detonation chamber test case*, 3rd European LS-DYNA Users Conference.

Kingery C. and Bulmarsh G. (1984). *Airblast Parameters from TNT Spherical Air Burst and Hemispherical Surface Burst*, ARBRL-TR-02555, U.S. Army Ballistic Research Laboratory, Aberdeen Proving Ground, MD.

Lacome J.-L. (2000). *Smooth Particle Hydrodynamics (SPH): A New Feature in LS-DYNA*, 6th International LS-DYNA Users Conference.

Lacome J.-L. (2008). *Analysis of Mine Detonation, SPH analysis of structural response to anti-vehicles mine detonations*. (DRDC Valcartier CR 2008-003). Defence R&D Canada Valcartier. Limited Distribution.

Larsen M. B. and Jorgensen K. C. (2007). *Landmine protection of armoured personnel carrier M113*, 6th European LS-DYNA Users Conference.

Li W.-C., Yu W.-F. and Cheng D.-S. (2007). *Increasing initial internal energy of air elements near explosive for fluid-structure models of a steel plate subjected to non-contact explosion*, 6th European LS-DYNA Users Conference.

LS-DYNA Theory Manual (2006). Livermore Software Technology Corporation, Livermore.

LS-DYNA Keyword User's Manual Version 971 (2007). Livermore Software Technology Corporation, Livermore.

Lucy L.B. (1977). *A numerical approach to the testing of the fission hypothesis,* The Astronomical Journal.

Mahmadi K., Aquelet N. and Souli M. (2002). *ALE Multi-Material Formulation of High Explosive Detonation using LS-DYNA3D,* ASME 2002, Emerging Technologies in Fluids, Structures, and Fluid/Structure Interactions, PVP-Vol. 446-1.

Martec Limited (2005). *Numerical Simulation of LAV III Rear Suspension.* (DRDC Valcartier CR 2006-596). Defence R&D Canada Valcartier. Unclassified.

Martec Limited (2007). *Numerical Study of Soil Modelling Approaches using LS-DYNA*. (DRDC Valcartier CR 2008-005). Defence R&D Canada Valcartier. Unclassified.

Morten R. J. (2008). Personal communications, LSTC.

Mullin M. J. and O'Toole B. J. (2004). *Simulation of energy absorbing materials in blast loaded structures*, 8th International LS-DYNA Users Conference.

Randers-Pehrson G. and Bannister K. (1997). Airblast Loading Model for DYNA2D and DYNA3D, ARL-TR-1310, Army Research Laboratory, Aberdeen Proving Ground, MD.

Slavik T. P. (2009-A). *A Coupling of Empirical Explosive Blast Loads to ALE Air Domains in LS-DYNA*, 7th European LS-DYNA Conference, LSTC.

Slavik T. P. (2009-B). Personal communications, Livermore Software Technology Corporation.

Toussaint G. and Durocher R. (2008). *Finite Element Simulation using SPH Particles as Loading on Typical Light Armoured Vehicles*, 10th International LS-DYNA Users Conference.

Tremblay J. E. (1998). *Impulse on Blast Deflectors from a Landmine Explosion*. (DREV TM-9814. Defence R&D Canada Valcartier. Unclassified.

Vulitsky M. Z. and Karni Z. H. (2002). *Ship Structures subject to high explosive detonation*, 7th International LS-DYNA Users Conference.

Wang J. (2001). *Simulation of Landmine Explosion Using Ls-Dyna3d Software: Benchmark Work of Simulation of Explosion in Soil and Air. DSTO-TR-1168.* Aeronautical and Maritime Research Laboratory.

Westine P.S., Morris B.L., Cox P.A and Polch E.Z. (1985).*Development of Computer Program for Floor Plate Response from Land Mine Explosions*, Technical Report No. 13045, US Army Tank-Automotive Command, Warren, MI.

Williams K. (1999). *Floor Deflection of the LAV-III Caused by the Detonation of a 7.5 Kg Anti-Tank Mine Surrogate*. Report to Diesel Division, General Motors of Canada Ltd. (DDGM) by Defence R&D Canada Valcartier. DREV TM-1999-154. Protected B, Limited Distribution.

Williams K. and Poon K. (2000). *A Numerical Analysis of the Effect of Surrogate Anti-Tank Mine Blasts on the M113*. (DREV TM-2000-007). Defence R&D Canada Valcartier. Unclassified.

Williams K. and Fillion-Gourdeau F. (2002). *Numerical Simulation of Light Armoured Vehicle Occupant Vulnerability to Anti-Vehicle Mine Blast*, 7th International LS-DYNA Users Conference.

Williams K., McClennan S., Durocher R., St-Jean B. and Tremblay J. (2002). *Validation of a Loading Model for Simulating Blast Mine Effects on Armoured Vehicles*, 7th International LS-DYNA Users Conference.

www.martec.com

Annex A ALE parametric study

The objective was to find the best combination of parameters that avoid or limit the leakage[3] in the mock-up ALE model. The different parameters studied were: NQUAD, DIRECT, PFAC, FRCMIN, ILEAK and PLEAK. The definitions of these parameters are given in the LS-DYNA Keyword User's Manual [2007] and are listed below:

NQUAD: Number of coupling points distributed over each coupled Lagrangian surface segment.

CTYPE: Fluid-Structure coupling method.

DIRECT: Coupling direction.

PFAC: Penalty factor.

FRCMIN: Minimum volume fraction of a coupled ALE multi-material group or fluid in a multi-material ALE element to activate coupling.

ILEAK: Coupling leakage control flag.

IPLEAK: Leakage control penalty factor.

Table A-1 shows the different parameter combinations and the yellow row gives the best set of parameters that was used in the ALE numerical results. It was suggested in the *LS-DYNA Keyword User's Manual* [2007] to set FRCMIN between 0.1 and 0.3 in hypervelocity cases, so FRCMIN was set to 0.1 since it turns on coupling earlier which helps preventing leakage.

*Table A-1: *Constrained_lagrange_in_solid parameters study*

NQUAD	CTYPE	DIRECT	PFAC	FRCMIN	ILEAK	IPLEAK	Leakage
3	4	default	0.2	0.3	default	default	a lot
3	4	3	0.2	0.3	default	default	very little
3	4	3	0.2	default	default	default	very little
3	4	default	0.2	0.1	default	default	a lot
3	4	2	0.2	default	default	default	some
3	4	2	0.2	0.3	default	default	some
3	4	2	0.2	0.1	default	default	some
4	4	2	0.2	0.1	default	default	a lot
4	4	2	0.2	0.3	default	default	a lot
4	4	2	0.2	default	default	default	a lot
4	4	2	0.2	0.1	2	0.2	a lot
3	4	3	0.2	0.1	2	0.2	N/A

[3] Leakage appears when the material flow passes through some of the elements of the Lagrangian mesh.

List of symbols/acronyms

ALE	Arbitrary Lagrangian Eulerian / Lagrangienne Eul□rienne arbitraire
DND	Department of National Defence
DRDC	Defence Research and Development Canada
DRDKIM	Director Research and Development Knowledge and Information Management
EEI	Engin explosif improvis□
EF	□l□ments finis
FE	Finite element
hr / hrs	Hour / Hours
IED	Improvised explosive device
LAV	Light armoured vehicle
min	Minutes
RDDC	Recherche et d□veloppement pour la d□fense Canada
R&D	Research and Development / Recherche et d□veloppement
SPH	Smoothed particle hydrodynamics / Hydrodynamique des particules lisses
VBL	V□hicule blind□l□ger
L/D	Length / Diameter
ρ	Mass density
ν	Poisson□s ratio
G	Shear modulus
E	Young□s modulus
σ_y	Yield stress
ETAN	Tangent modulus
FS	Failure strain
V_y	Velocity in the horizontal direction
V_z	Velocity in the vertical direction

DOCUMENT CONTROL DATA

(Security classification of title, body of abstract and indexing annotation must be entered when the overall document is classified)

1. ORIGINATOR (The name and address of the organization preparing the document. Organizations for whom the document was prepared, e.g. Centre sponsoring a contractor's report, or tasking agency, are entered in section 8.)

Defence R&D Canada – Valcartier
2459 Pie-XI Blvd North
Quebec (Quebec)
G3J 1X5 Canada

2. SECURITY CLASSIFICATION (Overall security classification of the document including special warning terms if applicable.)

UNCLASSIFIED

3. TITLE (The complete document title as indicated on the title page. Its classification should be indicated by the appropriate abbreviation (S, C or U) in parentheses after the title.)

Comparison of ALE and SPH methods for simulating mine blast effects on structures

4. AUTHORS (last name, followed by initials – ranks, titles, etc. not to be used)

Toussaint, G.; Bouamoul, A.

5. DATE OF PUBLICATION (Month and year of publication of document.)

December 2010

6a. NO. OF PAGES (Total containing information, including Annexes, Appendices, etc.)

50

6b. NO. OF REFS (Total cited in document.)

25

7. DESCRIPTIVE NOTES (The category of the document, e.g. technical report, technical note or memorandum. If appropriate, enter the type of report, e.g. interim, progress, summary, annual or final. Give the inclusive dates when a specific reporting period is covered.)

Technical Report

8. SPONSORING ACTIVITY (The name of the department project office or laboratory sponsoring the research and development – include address.)

Defence R&D Canada – Valcartier
2459 Pie-XI Blvd North
Quebec (Quebec)
G3J 1X5 Canada

9a. PROJECT OR GRANT NO. (If appropriate, the applicable research and development project or grant number under which the document was written. Please specify whether project or grant.)

12ro03

9b. CONTRACT NO. (If appropriate, the applicable number under which the document was written.)

10a. ORIGINATOR'S DOCUMENT NUMBER (The official document number by which the document is identified by the originating activity. This number must be unique to this document.)

DRDC Valcartier TR 2010-326

10b. OTHER DOCUMENT NO(s). (Any other numbers which may be assigned this document either by the originator or by the sponsor.)

11. DOCUMENT AVAILABILITY (Any limitations on further dissemination of the document, other than those imposed by security classification.)

Unlimited

12. DOCUMENT ANNOUNCEMENT (Any limitation to the bibliographic announcement of this document. This will normally correspond to the Document Availability (11). However, where further distribution (beyond the audience specified in (11) is possible, a wider announcement audience may be selected.))

Unlimited

13. ABSTRACT (A brief and factual summary of the document. It may also appear elsewhere in the body of the document itself. It is highly desirable that the abstract of classified documents be unclassified. Each paragraph of the abstract shall begin with an indication of the security classification of the information in the paragraph (unless the document itself is unclassified) represented as (S), (C), (R), or (U). It is not necessary to include here abstracts in both official languages unless the text is bilingual.)

Defence Research and Development Canada Valcartier (DRDC Valcartier) has been developing protection systems for many years to reduce the vulnerability of light armoured vehicles (LAV) against mine blast. To assist in the development of these protections, experimental tests and finite element (FE) analyses are performed. To carry out these numerical calculations, initial conditions such as the loading prescribed by a mine on a structure need to be simulated adequately. The effects of blast on structures depend often on how these initial conditions are estimated and applied. In this report, two methods were used to simulate a mine blast: the arbitrary Lagrangian- Eulerian (ALE) and the smoothed particle hydrodynamics (SPH) formulations. The comparative study was done for a simple and a more complex target.

The first target is an aluminum plate placed on four steel legs and centred over a surrogate mine filled with 6 kg of C4 which represents a typical buried mine blast scenario. Two FE models were generated: an ALE model and a SPH model. The final deformation of the plate was measured for both approaches and was compared with experimental measurements.

The second target is a mock-up, representing a section of the side of a typical LAV, subjected to a typical improvised explosive device (IED). Two FE models were generated: an ALE model and a SPH model. Parametric studies were done on both models and the best results were compared to the experimental ones. Each comparison included the velocity at the center of the sponson wall, sponson top and sponson sidewall.

14. KEYWORDS, DESCRIPTORS or IDENTIFIERS (Technically meaningful terms or short phrases that characterize a document and could be helpful in cataloguing the document. They should be selected so that no security classification is required. Identifiers, such as equipment model designation, trade name, military project code name, geographic location may also be included. If possible keywords should be selected from a published thesaurus, e.g. Thesaurus of Engineering and Scientific Terms (TEST) and that thesaurus identified. If it is not possible to select indexing terms which are Unclassified, the classification of each should be indicated as with the title.)

Blast, Arbitrary Lagrangian Eulerian, ALE, Smoothed particle hydrodynamics, SPH, Explosive, Mock-up, IED

Defence R&D Canada

Canada's Leader in Defence
and National Security
Science and Technology

R & D pour la défense Canada

Chef de file au Canada en matière
de science et de technologie pour
la défense et la sécurité nationale

www.drdc-rddc.gc.ca